Autofocus system for space cameras

Zhaohui Li
Keyong Wu
Chinese Academy of Sciences
Changchun Institute of Optics, Fine Mechanics and Physics
Changchun 130022, China
E-mail: lizh_ciom@yahoo.com.cn

Abstract. A novel autofocusing technique using a self-imaging approach is developed for a space camera having large aperture and long focus. Its optical system consists of an emitting system, receiving system, and two pentagonal prisms. The emitting system has three parts: a light source, beamsplitter, and aim slit. The receiving system includes a field lens, two separate lenses, and CCD. Using two little pentaprisms instead of a large planar mirror makes the autofocus system simple and compact. A defocused signal is acquired by measuring the change of the slit self-image position imaged on the CCD. The algorithm to calculate the movement of the slit self-image position is analyzed to achieve subpixel position estimation. The results of the experiments show a ± 10-μm precision of autofocusing in a range of ± 5-mm defocusing. The system demonstrates high resolution, easy adjustment, and high reliability. Also this method can meet the requirements of various accurate focus measurement systems.
[DOI: 10.1117/1.1901686]

Subject terms: autofocus; space camera; self imaging; pentaprisms.

Paper 040137 received Mar. 15, 2004; revised manuscript received Sep. 7, 2004; accepted for publication Nov. 30, 2004; published online May 10, 2005.

1 Introduction

The autofocusing technique is one of the commonly used techniques for space cameras to ensure a high-quality image. The focal plane of the camera goes beyond the permitted bounds due to many influential factors, such as the influence of the impulsion or jitter in the process of launching, changes of temperature and air pressure, changes on the surface of the lens and refractive index, etc. Although some compensation such as thermoregulation and material matching technology are used in space cameras, spatial resolution cannot be improved if focusing is not done before photographing.

Three main autofocusing methods applied to space cameras are: program operating, image processing, and photoelectric autocollimation methods. For program operating methods, defocus amount-temperature-air pressure correlations need to be determined, which are carried out according to the parameters of temperature and air pressure from the sensors in the camera. The condition used in this method may not exactly represent the real space circumstance. Image processing methods are just applied in electronic transmitted cameras. In this approach, typically a focus measurement is performed by computing images acquired at several different lens positions, and the lenses are moved to the position where the evaluation function becomes extreme. The last method utilizes the full aperture of the camera and represents the optimum focus to infinite object, so it is adopted widely in measuring focal lengths for large optical instruments.

The photoelectric autocollimation method requires a high-quality planar mirror with large aperture, which increases the weight of the camera and adds many difficulties for the adjusting, fabricating, and control system. In addition, the vertical photographing space camera does not allow placement of a planar mirror in front of the camera lens. In this work, an alternative technique is developed, where two little pentagonal prisms replace the large planar mirror. The pentaprism has the property of reflecting rays at right angles. The property turns the measuring defocus along the axis to radial measurement, and the vertical measurement is sensitive. This system can adjust easily and has a compact diminutive structure: its accuracy is within 10 μm with a measurement range of ± 5 mm.[1-6]

0091-3286/2005/$22.00 © 2005 SPIE

2 Results and Discussion

2.1 *Principle of Autofocusing*

2.1.1 *Optical configuration*

The principle of the self-imaging technique is shown in Fig. 1. The optical path of the focusing system contains the emitting system, receiving system, pentagonal prism assembly, and signal process unit. The emitting system consists of the light source, beamsplitter, and slit. The receiving system consists of a field lens, two separate lenses, and CCD. The position of the slit and image plane of the camera are the conjugate plane, and the field lenses are coplanar with the slit.

2.1.2 *Principle*

In Fig. 1, the two pentaprisms are placed along a radius in front of the camera aperture. The two right-angled surfaces of the pentaprism are an output plane: on the other hand, they are also an input plane. First, a light source collimated by an objective is divided into two beams by a split prism and illuminates the slit. The slit is imaged by a camera optical system on the pentagonal prisms. Second, the two images of the slit are reflected by the pentaprisms, then go through the camera optical system again and are reimaged by two separate lenses on a CCD, respectively. Finally, the

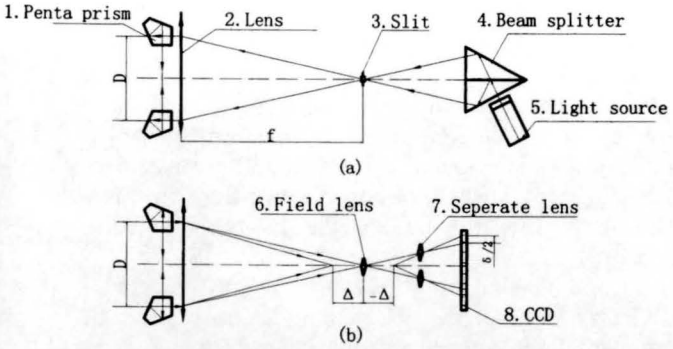

Fig. 1 Schematic diagram of the focusing system: (a) emitting system and (b) receiving system.

two slit self-images are converted into a digital signal, and the defocusing amount is determined by calculating the displacement between the two slit images.

2.1.3 *Relationship between defocus and the displacement of two slit self-images*

When the camera system defocuses an amount of $\pm\Delta$, each of the two slit self-images will generate a displacement $\pm\delta/2$ along the CCD. The relation between δ and Δ can be determined based on the theory of geometrical optics:

$$\delta = -\frac{\Delta M D}{f'}, \tag{1}$$

$$\Delta = -\frac{\delta F}{M}, \tag{2}$$

where D is the distance between the two pentagonal prisms in front of the camera, the magnification of the separate lens is M, f' is the focal length, and F is the f number of the camera. The minus denotes the direction of defocus.

2.1.4 *Analysis of sensitivity*

As shown in Eq. (2), the displacement of the two slit self-images on the CCD is proportional to the defocused amount. If $F=5.6$, the CCD pixel space is 7 μm and $M=2$. The focusing resolution is $\Delta=19.6$ μm.

The depth from focus of a camera is $\Delta_z=2\lambda F^2$. The resolution $\Delta=19.6$ μm is not sufficient. It is necessary to adopt digital signal processing technology. Certainly, increasing magnification M can improve the resolution, but it will enlarge focusing system construction and decrease incidence energy.

2.1.5 *Calibration*

This focusing approach requires measuring the distance between the two slit self-images when the camera is focused on an optimized level. In other words, the origin in the relative coordinate for setting up the basis of comparing with other environments is investigated.

Here we use a parallel light pipe with 30-m focal length and a large vacuum tube to measure the optimal focus in the laboratory.

The calibration error influences the focusing precision, but the focus position is measured relatively in this method. Reproducibility precision rather than absolute accuracy is more important.

2.2 *Algorithm for Estimating the Displacement of Slit Images*

2.2.1 *Analysis of the algorithm*

According to the focusing principle, the key issue is to estimate the locations of the slit self-images to calculate the displacement between the two slit self-images on the CCD. To reach the expected focus resolution, a subpixel processing approach needs to be used. Several typical approaches to detect spot position are centroid sensing, energy distribution fitting, and correlative methods. Centroid sensing and fitting methods are perfect for the signal with regulative and homogeneous energy distributions. The correlation method has some statistical characteristics, and statistical processing for light spots helps to reduce random noise, the influence of nonuniformity of light, and the CCD response.

As mentioned previously, since the two slit self-images are similar, the correlation peak of the two light signals can be calculated, and the shift of the peak point versus the movement of the two light spots can be obtained using Eq. (2).

2.2.2 *Comparison of correlative methods*

To compare the performance of the correlation algorithms, different types of correlative methods are discussed in this section.

The product correlation function is defined by:

$$R_P(k)=\sum_{n=1}^{N} x_1(n)\cdot x_2(n+k), \quad k=0,\pm 1,\pm 2,...\pm M,$$

where n is the number of sample points along the CCD, k is the shift of signal x_2 relative to x_1, and $x_1(n)$, $x_2(n)$ are the discrete digital signals for $n=1,2,...N$.

The mean square difference (MSD) correlation function is given by:

$$R_S(k)=\sum_{n=1}^{N} |x(n)-x_2(n+k)|^2,$$

and the mean absolute difference (MAD) correlation function is expressed as:

$$R_L(k)=\sum_{n=1}^{N} |x(n)-x_2(n+k)|. \tag{3}$$

Equation (3) means that the sequence $x_1(n)$ compares with $x_2(n)$ that shift left units k. The minimum value is obtained when $x_1(n)$ and $x_2(n)$ are closest, then the movement δ is achieved.

2.2.3 *Simulation*

Using numerical simulation, the performance of MAD, MSD, and the product methods mentioned before are evaluated in a noise environment.

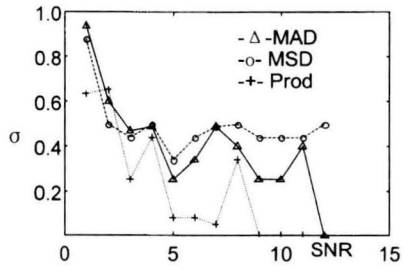

Fig. 2 The capability comparison of several correlation measurement methods.

An exponent function is proposed for characterizing the intensity distribution of the slit self-image:

$$E(x)=E_0\cdot\exp\left[-\frac{2(x-x_0)^2}{\rho^2}\right],$$

where E_0 is the maximal intensity, x_0 is the center position of the light spot, and ρ is the half width of the Gaussian spot.

To understand the effect of noise on the detection accuracy, we defined the signal-to-noise ratio (SNR) as:

$$\mathrm{SNR}=20\lg\frac{E_0}{\sigma_n},$$

where σ_n is the standard deviation of white noise.

The standard deviation σ of position location is used to characterize the reliability at various SNRs, such as 5, 10, 20 and ∞ dB, since σ represents the performance of reiteration and stability. The simulation results are shown in Fig. 2. It is found that the product has the highest precision, and MSD has the lowest.

Considering the computation speed and complexity, the MAD algorithm is employed in hard implementation of an algorithm.

2.3 *Design of the Autofocusing System*

2.3.1 *Design of the illuminated setup*

To make the illuminating beam fulfill the aperture of the pentaprism in front of the camera aperture, two optical setups are applied. In the first one, a semiconductor is employed as light source to produce a stripe by a cylinder lens. The main advantage of the laser beam is sufficient achievable incidence. The disadvantage is the high loss of the emitted power because the beams are magnified many times and only a small portion of incidence light can be collected by the pentaprism. Moreover, since the stripe is nonuniform in energy distribution, the electrical signal quality is poor.

In the second version, an LED with a flat-truncated package, which is equipped with a pinhole aperture, generates a semipoint light source, and the beams leaving the pinhole are collimated with an objective lens.

The design process strived to maximize the system energy and enhance the SNR. The emitting system employs a split prism to make two LEDs illuminate the slit simultaneously, therefore doubling the incident light energy. The two beams emitted from LEDs pass through the split prism, illuminate the slit, go through the camera optical system, and then they are incident on the pentaprism, respectively (Fig. 3). The dispersed angle of the two beams should match the position of the two pentaprisms located in front of the camera aperture.

2.3.2 *Design of receiving system*

The receiving system consists of a field lens located at the same plane with the slit, two separate lenses, and the CCD. The field lens serves to enhance the capability of lateral rays going into the receiving system. Its effective focus length (EFL) is $f'=26.6$ mm, $\phi=5$ mm. Taking into account the slit self-image width, position measuring accuracy, and arrangement in the space camera, the magnification of the separate lens in the receiving system is determined finally as $M=2$. The EFL of the separate lens is $f'=19.6$ mm, NA=0.1.

The CCD is selected as a photoelectric device (model IL-C7-4096, Dalsa Incorporated, Canada). After an amplifier, the signal is sampled, converted through an A/D converter, and stored in a RAM. It is processed by a microprocessor. The signal waves are shown on Fig. 3. The output signal after the power amplifier gives a step motor to drive a cam mechanism.

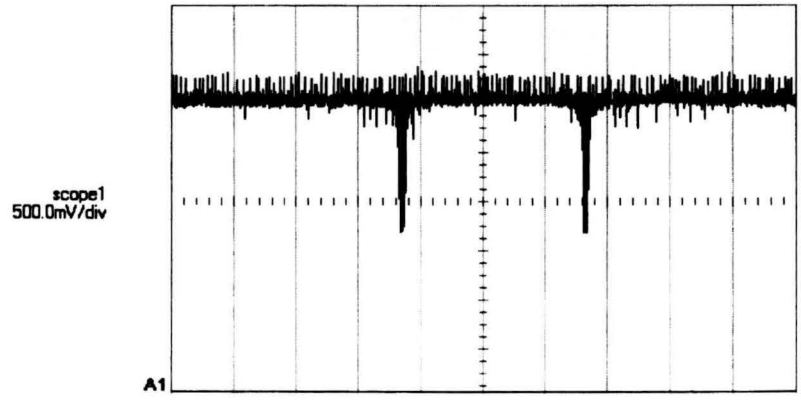

Fig. 3 The weave of two light signals showing on oscillograph HP54645D.

2.3.3 *Design of width of the slit self-image*

Considering the diffraction effect of the pentaprism and the magnification of the receiving system, the width of the slit self-image is calculated as:

$$\delta' = \left(\delta + \frac{\lambda}{\Delta} \phi' \right) M, \tag{4}$$

where d is the width of the slit, f' is the focal length of the camera, D is the aperture of the pentaprism, λ is the wavelength of the LED, and M is the magnification of the separate lens in the receiving system, as mentioned before as $M=2$.

The measurement of position of the slit self-image is the key to determining the focusing accuracy. The position estimating error is impacted by the slit width d'. From Eq. (4), d' is a function of D, d, and M. An optimized compromise would be made to enable the width of slit self-image d' to be suitable for measuring.

On one hand, to receive more energy, the pentaprism aperture D should be enlarged as high as possible. On the other hand, to avoid the pentaprism cutting into the camera optical system, it is necessary to limit the size of the pentaprism aperture. However, from Eq. (4), the smaller the size of D, the larger the obvious diffraction effect, which makes the signal occupy more CCD pixels. Parameter D was determined based on analysis and experiments in this work.

The width of the slit d is given similarly in compromise. If the slit is too narrow, it brings difficulties to the illuminating system design, and as a result, the signal energy is decreased. If the slit is too wide, it makes the grayscale variation of the slit image degrade, which makes the SNR decline. Optimizing must be done when designing the slit mode.

2.4 *Experimental Results and Analysis*

After the system was completed, tests were implemented on a prototype camera with EFL=2700 m, 1/F=5.6.

In our experiment setup, the focusing assembly was mounted on a precise x-y stage with minimal scale 0.01 mm. Positive or negative defocus can be obtained by turning the tub wheel of the x-y stage at each defocus position. The displacement of the two slit image was calculated. The test was performed ten times in every position, and the results are shown in Table 1.

Table 1 Displacement of the two-slit image.

Reading of the wheel Z (μm)	Defocus amount in theory Δ_z (μm)	Defocus amount by measured $\Delta=(F/M)\cdot\delta$	Standard deviation σ (μm)
10	−50	−45.2	3.34
20	−40	−42.6	2.43
30	−30	−34.6	2.70
40	−20	−24	2.65
50	−10	−13.3	1.44
60	0	0	1.07
70	10	10.6	1.98
80	20	18.6	2.30
90	30	26.6	2.50
100	40	40	2.11
110	50	48	3.85

The results show that a resolution of 0.01 mm is obtained with the measurement range of ± 5 mm. The standard deviation is $\sigma \leqslant 0.004$ mm. In our focus approach, it is expected to find the variable of the focal plane, not the true value of the defocus amount. So the absolute measurement error of the defocus amount is not significant, although it seems big. The newly designed autofocusing system in this work demonstrated the following characteristics.

The systematic error does not affect the focus accuracy. It shows the advantages, such as the higher reproducibility and resolution, easy adjustment, and compact structure.

The measuring uncertainty is mainly caused by the following factors: 1. light source waves in intensity and their distribution induce the reproducibility error of location; 2. photoelectric converts introduced fixed pattern noise, dark current noise, KTC noise (reset noise), and photoresponse nonuniformity, etc; 3. the sampling errors are due to the integer pixel; 4. adjustment is not perfect; and 5. some errors remain due to calibration.

The focusing system has no inherent systematic errors, but is limited by the random noise in the signal. When the wheel of the x-y stage turns half a minimal scale, which is 0.005 mm, the movement of the light spot is not detected, since the information of shift of the spot is indulged in random noise, as mentioned before.

3 Conclusion

The focusing method studied in this work proves to be an autofocusing method having high resolution, good iteration, and reliability. This device has a compact structure. The experiment results indicate that focusing precision can reach ± 0.01 mm. The system has high reliability and can meet the autofocusing requirements of various large aperture optical instruments.

Acknowledgments

The original concept was developed by C. Y. Han. The authors would like to acknowledge Z. X. Wang for his constructive work on the experiments. Thanks also go to J. Q. Wang who provided a prototype camera with a large aperture and long focus.

References

1. S. Xue and Q. Li, *Design of Precision Instruments*, pp. 230–240, Tsinghua University Press, Beijing, China (1990) [in Chinese].
2. P. Jennison and L. G. Gregoris, "A self imaging technique for focusing an IR telescope," *Proc. SPIE* **1309**, 245–256 (1990).
3. A. W. Lohmann and D. Mendlovic, "Digital method for measuring the focus error," *Appl. Opt.* **36**(28), 7204–7209 (1997).
4. M. Subbarao and J. K. Tyan, "Selecting the optical focus measure for autofocusing and depth-from-focus," *IEEE Trans. Pattern Anal. Mach. Intell.* **20**(8), 864–870 (1998).
5. D. K. Cohen, W. H. Gee, M. Ludeke, and J. Lewkowicz, "Automatic focus control: the astigmatic lens approach," *Appl. Opt.* **23**(4), 565–570 (1984).
6. L. Subbarao, "Focusing techniques," *Opt. Eng.* **32**(11), 2824–2836 (1993).

Zhaohui Li is a research associate at the Changchun Institute of Optics, Fine Mechanics, and Physics, Chinese Academy of Sciences. He received his BS and MS degrees from Changchun University of Technology in 1991 and 1994, respectively. He received the PhD from Changchun Institute of Optics, Fine Mechanics, and Physics, Chinese Academy of Sciences, in 2001. His main research interests are optoelectricity instrument design and analysis.

Keyong Wu graduated from the optical engineering department of Changchun Institute of Optics and Fine Mechanics in 1964. He is now a senior researcher at Changchun Institute of Optics, Fine Mechanics, and Physics, Chinese Academy of Sciences. His research activities include optical engineering, optical instruments, and photoelectricity meterage.